Efficient Simulation and Acceleration of Convergence for a Dual Piston Pressure Swing Adsorption System

Efficient Simulation and Acceleration of Convergence for a Dual Piston Pressure Swing Adsorption System

Daniel Friedrich, Maria-Chiara Ferrari, Stefano Brandani*

Scottish Carbon Capture and Storage Centre, School of Engineering
The University of Edinburgh, The King's Buildings, Mayfield Road
Edinburgh EH9 3JL. UK
s.brandani@ed.ac.uk

Industrial and Engineering Chemistry Research, 53, 26, p. 8897-8905, 2013

Abstract

The Dual Piston Pressure Swing Adsorption (DP-PSA) system offers the potential for the full characterisation of adsorbent materials under a large range of experimental conditions. The analysis of these experiments requires an efficient tool for the simulation of the DP-PSA system to Cyclic Steady State (CSS). In this contribution a simulation tool is developed and applied to a mathematical model of the DP-PSA system. The governing set of Partial Differential Equations (PDEs) is solved with state-of-the-art discretisation schemes, which are tailored to the character of the governing equations. PDEs with a strong hyperbolic character are discretised with the Finite Volume Method (FVM) with a flux-limiting scheme; this guarantees the conservation of mass as well as correct tracking of the moving fronts. The mass transfer in the adsorbent materials is discretised with the orthogonal collocation on finite elements method which is a very efficient method for problems with steep, stationary gradients. The large system of Differential Algebraic Equations (DAEs) is solved with the state-of-the-art DAE solver SUNDIALS. Even with these sophisticated discretisation schemes, the computation times to reach CSS are long due to the non-linear system behaviour as well as the complex nature of the system. Several strategies to reduce the computation time are implemented: i) conservative node refinement: initial simulation with lower resolution discretisation; ii) implementation of numerical acceleration schemes, e.g. extrapolation method, which accelerate the convergence to CSS; iii) restart from previous

simulation runs. Each of the acceleration schemes reduces the required simulation time by at least a factor of 2 and the combination of the schemes accelerates the simulation by a factor of 10. Thus the combined simulation tool allows the rapid simulation of the DP-PSA system.

Keywords: Pressure swing adsorption; fast cycles; numerical simulation; cyclic steady state; acceleration; interpolation; extrapolation; ε algorithm

1. Introduction

Adsorption based separations such as pressure swing adsorption (PSA) and vacuum swing adsorption (VSA) have large potential for many separation processes ranging from portable oxygen concentrators to CO_2 capture units for commercial Carbon Capture and Storage (CCS) application in power plants and industry. Carbon capture research is developing rapidly due to the ambitious CO_2 reduction targets and the large energy penalty of the first generation capture technology, i.e. liquid amine-based absorbents.[1] Adsorption based processes have the potential to lower the energy penalty and to achieve higher productivity.[2] The latter is further enhanced by the move to faster cycles and thus to smaller separation units.

To achieve an efficient and cost-competitive adsorption based separation process requires the optimisation of the adsorbent materials and process conditions to the specific separation. Both aspects contain a large number of parameters: i) the characteristics of novel adsorbent materials, such as kinetic and equilibrium parameters, have to be estimated from experiments; ii) the adsorption process depends critically on the process conditions, such as cycle configuration, column and adsorbent sizes, temperature, pressure and flow rates. Hence a solely experimental approach is not feasible and it is important to support experiments by accurate and efficient simulation tools. These computational tools have to be built from models which accurately describe the underlying physical processes. Once these tools are validated they can be used for the parameter estimation for novel adsorbents and for the optimisation of the process conditions.

The Dual Piston Pressure Swing Adsorption (DP-PSA) system first described by Keller and Kuo[3] allows independent control of pressure and flow in the adsorption column. Briefly, a DP-PSA system consists of two independently controlled piston-cylinder assemblies which are connected to a column

filled with a suitable adsorbent material. While it has been shown that this configuration increases the separation performance, this setup is also uniquely suited for the testing and characterisation of novel adsorbents under a wide variety of process conditions. Potential process conditions include different cycle configurations (stroke length, phase angle, cycle times) and starting pressures and composition. Furthermore, by enclosing the DP-PSA in an oven and running it as a closed system hundreds of different experiments can be run in an automatic way. The key advantages of using a DP-PSA system as an experimental technique to characterise adsorption columns are:

1) The ability to change cycle times easily, enabling to test the separation efficiency at cycle times of a few seconds, which are needed for example in carbon capture applications;
2) The possibility to run the system at total reflux, i.e. in a closed configuration, which enables the users to test the columns without consuming gases.

Thus the interpretation of the results from these experiments requires an accurate, reliable and fast simulation tool.

Several simulation tools for cyclic adsorption processes in general[4, 5] and piston-driven in particular[6-8] have been developed in recent years. However, due to the large number of possible experiments in the DP-PSA system there is a need for a simulation tool which accurately describes the adsorption process over a wide range of experimental conditions and is strictly conservative given that the DP-PSA is run at total reflux. A further challenge, given the potential use of nonlinear regression algorithms to determine model parameters directly from the DP-PSA experiments, is the requirement for fast convergence to Cyclic Steady State (CSS). Like most adsorption processes the DP-PSA system is run in a cyclic manner and will reach CSS after a certain number of cycles; under non-isothermal conditions CSS is often reached only after hundreds or even thousands of cycles.[5] The normal approach is to simulate one cycle after the other in the so called successive substitution method. However, the convergence of this method is only linear.[9] In recent years several methods have been employed to

decrease the required computational time: complete discretisation of the spatial and temporal domain;[10] extrapolation using Newton's method;[11] model switching;[5] and node refinement.[12]

In this paper we are presenting the development of an efficient simulation tool for the DP-PSA system. An established mathematical model is extended with a pore diffusion model and the resulting PDEs are discretised with tailored numerical schemes. The resulting set of differential equations is solved with the Backward Differentiation Formula implemented in the SUNDIALS solver suite. Furthermore, several strategies ranging from extrapolation methods to interpolation methods are presented. The combination of tailored discretisation and acceleration strategies yields a fast simulation tool.

2. Mathematical model

A schematic of the DP-PSA system modelled is shown in Figure 1; this system consists of two pistons-cylinder assemblies (henceforth called pistons) connected to either side of one column. The governing equations for the pistons and the column will be described separately and linked together through boundary conditions. The column model is implemented as an independent unit, which is the basis for a general cycle simulator which can then be used to predict the performance of adsorption separation processes.

The mathematical model used here follows the model developed by Singh and Jones,[8] Farooq et al.[7] and Rajendran et al.[6] for the simulation of piston-driven adsorption processes and adds a pore diffusion model for the mass transfer in the adsorbent particle. Thus the mass transfer in the adsorbent particle can be simulated either by the Linear Driving Force (LDF) model or by pore diffusion. These two models form the basis for the development of a model hierarchy of increasing complexity, which can

be used to describe the mass transfer in the particles. For the purposes of the present contribution, as will be shown in the comparison with preliminary DP-PSA results, the both the LDF and macropore diffusion models capture accurately the behaviour of the system. The column model can be extended further to include several options for the description of the mass, momentum and energy balance.

The mathematical model is based on the following assumptions:

1. Axial dispersed plug flow
2. Momentum balance: no pressure drop
3. Energy balance: isothermal operation
4. Mass transfer: i) Linear driving force (LDF) model or ii) pore diffusion
5. Adsorption isotherm: i) linear or ii) Langmuir
6. The gas concentrations in the pistons are assumed to be uniform
7. The dead volume is distributed equally among the two cylinders
8. No flow resistance between the pistons and column
9. Ideal gas law

The resulting models are sufficiently complex and nonlinear to allow to study the implementation of state-of-the-art discretisation and accelerated convergence to CSS approaches.

2.1 Governing equations for the column

The flow along the length of the column is assumed to be axial dispersed plug flow with a uniform concentration profile in the radial direction. From this the component mass balance along the column is given by

$$\frac{\partial c_i}{\partial t} + \frac{(1-\varepsilon)}{\varepsilon} \cdot \frac{\partial Q_i}{\partial t} + \frac{\partial (v \cdot c_i)}{\partial z} + \frac{\partial J_i}{\partial z} = 0 \quad i = 1,\ldots,N_c \tag{1}$$

Assuming that the gas is ideal, the isothermal mass balance can be rewritten as

$$c_T \frac{\partial y_i}{\partial t} + c_T \frac{y_i}{P}\frac{dP}{dt} + \frac{(1-\varepsilon)}{\varepsilon} \cdot \frac{\partial Q_i}{\partial t} + \frac{\partial (v \cdot y_i)}{\partial z} + \frac{\partial J_i}{\partial z} = 0 \quad i = 1,\ldots,N_c \tag{2}$$

Summing over all components

$$\frac{1}{P}\frac{dP}{dt} + \frac{\partial v}{\partial z} + \frac{(1-\varepsilon)}{\varepsilon c_T}\sum_{i=1}^{N_c} \frac{\partial Q_i}{\partial t} = 0 \tag{3}$$

where y_i is the mole fraction of component i in the fluid phase, ε is the bulk void fraction and v the interstitial velocity. Here and from now on the index i goes from 1 to the number of components N_c. The mean adsorbed concentration Q_i and the diffusive flux J_i are given by

$$Q_i = \frac{3}{r_p}\int_0^{r_p} q_i r^2 dr \tag{4}$$

$$J_i = -D_i c_T \frac{\partial y_i}{\partial z} \tag{5}$$

where r_p is the adsorbent particle radius, D_i the axial dispersion coefficient, c_T the total fluid concentration and y_i the mole fraction of component i. The mass transfer in the adsorbent particle can either be described by the LDF model

$$\frac{dq_i}{dt} = k_i \frac{3}{r_p}\left(q_i^* - q_i\right) \tag{6}$$

or by the pore diffusion model

$$\frac{\partial q_i}{\partial t} + \frac{1}{r^2}\frac{\partial}{\partial r}\left(-D_i^e r^2 \frac{\partial q_i}{\partial r}\right) = 0$$
$$q_i\big|_{r=r_p} = q_i^* \qquad (7)$$
$$\left.\frac{\partial q_i}{\partial r}\right|_{r=0} = 0$$

Here q_i^* is the sorbate concentration in the adsorbent particle at equilibrium, k_i is the LDF mass transfer coefficient and D_i^e is the effective pore diffusivity. The equilibrium value depends on the used adsorption isotherm. Here the linear or multi-component Langmuir isotherms are considered. The Langmuir isotherm is given by

$$q_i^* = \frac{q_{s,i} b_i P y_i}{1 + \sum_{j=1}^{N_c} b_j P y_j} \qquad (8)$$

where $q_{s,i}$ is the saturation capacity and b_i is the Langmuir constant.

To close the mass balance in the column the Danckwerts boundary conditions are used. These can be written concisely as

$$J_i\big|_{z=0} = \frac{v_1 + |v_1|}{2}\left(y_{i,0-} - y_i(0)\right)c_T$$
$$J_i\big|_{z=L} = \frac{v_2 - |v_2|}{2}\left(y_{i,L+} - y_i(L)\right)c_T \qquad (9)$$

The velocities at the column boundaries are calculated from the total mass balance in the DP-PSA system. Initially the column is at a uniform pressure and gas phase concentration and the adsorbent material is assumed to be in equilibrium with the set gas phase concentration.

2.2 Governing equations for the pistons

Each piston performs a sinusoidal cycle and thus the piston position can be described by the following

equation

$$S(t) = S_{0,j} + \frac{S_{1,j} - S_{0,j}}{2}\left(1 - \cos\left(\omega t + \varphi_j\right)\right) \tag{10}$$

where $S_{0,j}$ and $S_{1,j}$ are the start and end position of the piston, respectively, $\omega = 2\pi/t_c$ is the cycle frequency and φ the initial piston offset. From this the piston volume is calculated by $V_{p,j} = \pi R_p^2\left(L_p - S(t)\right)$. The combined dead volumes in the connecting lines and between the fully extended piston and the cylinder head are given by $V_{D,j} = \pi R_p^2\left(L_p - S_{1,j}\right)$.

The material balance for pistons 1 and 2 is given by

$$\begin{aligned}\frac{dy_{i,p1}}{dt} &= \frac{v_1 - |v_1|}{2V_{p,1}}\left(y_{i,p1} - y_i(0)\right)\\ \frac{dy_{i,p2}}{dt} &= \frac{v_2 + |v_2|}{2V_{p,2}}\left(y_i(L) - y_{i,p2}\right)\end{aligned} \tag{11}$$

2.3 Pressure and flow velocity

The mathematical model of the DP-PSA system assumes that the pressure is spatially uniform in the complete system. While this is not generally accurate, the purpose of this paper is not the development of the most accurate model for the DP-PSA system but the development of efficient and fast simulation methods. With the assumption of uniform pressure and from the overall mass balance around the two pistons expressions for the flow velocity at the left and right of the column can be derived

$$\begin{aligned}v_1 &= -\frac{V_{p,1}}{P\varepsilon\pi R^2}\frac{dP}{dt} - \frac{1}{\varepsilon\pi R^2}\frac{dV_{p,1}}{dt}\\ v_2 &= \frac{V_{p,2}}{P\varepsilon\pi R^2}\frac{dP}{dt} + \frac{1}{\varepsilon\pi R^2}\frac{dV_{p,2}}{dt}\end{aligned} \tag{12}$$

Replacing the velocity derivative in the overall mass balance with the average velocity gradient along the column length yields an expression for the pressure in the system

$$\frac{1}{P}\frac{dP}{dt} = \frac{1}{L}\left[v_1 - v_2 - \frac{(1-\varepsilon)}{\varepsilon c_T}\sum_{i=1}^{N_c}\int_0^L \frac{\partial Q_i}{\partial t} dz \right] \tag{13}$$

3. Numerical solution strategy for the mathematical model

Due to the complexity, nonlinearity and inherent dynamic nature of the DP-PSA system the mathematical model introduced in the last section has to be solved numerically. The governing Partial Differential Equations (PDE) are discretised in space with discretisation schemes tailored to the properties of the equations in the fluid and solid phase, respectively. The resulting large set of Differential Algebraic Equations (DAE) is solved with the DAE solver suite SUNDIALS.[13]

3.1 Fluid phase spatial discretisation

The fluid phase is discretised with the Finite Volume Method (FVM) which is inherently conservative and therefore well suited for the discretisation of conservation laws. This is particularly important for the DP-PSA system operated at total reflux since the system is closed and any inconsistency or even small non-conservative error will build up and eventually cause the simulation to fail. The PDEs in the fluid phase are typically dominated by the convective term and thus present a strong hyperbolic character. Together with usually favourable isotherms this leads to the formation and propagation of shocks along the column. It is thus necessary to use specialised discretisation schemes which take the shock propagation into account. Here we are using a flux-limited FVM[14] with the van Leer flux limiter. This method uses a higher order discretisation in the smooth regions of the solution and the unconditionally stable first order upwind method close to the shock.

In the FVM the spatial domain is split into a finite number N of cells and the conservation law is enforced on each of these volume elements; see figure 2.

In our implementation it is assumed that the state variable is constant over the finite volume and this average value is stored at the centre node. More complex approximations inside the finite volumes are possible but the approximation used has 2nd order accuracy in accordance with the accuracy of the evaluation of the cell boundary fluxes. The spatial derivatives, i.e. the convection and axial dispersion term, are approximated by cell-centred differences. Thus each mass balance PDE along the column is discretised into N ordinary differential equations (ODE)

$$\frac{\partial \bar{y}_{i,j}}{\partial t} + \frac{\bar{y}_{i,j}}{P}\frac{dP}{dt} + \frac{(1-\varepsilon)}{\varepsilon c_T}\cdot\frac{\partial Q_{i,j}}{\partial t} + \frac{F_{i,j+1/2} - F_{i,j-1/2}}{\Delta z} + \frac{J_{i,j+1/2} - J_{i,j-1/2}}{\Delta z} = 0 \qquad (14)$$
$$i = 1,\ldots,N_c, j = 1,\ldots,N$$

The cell boundary fluxes are interpolated from the nodal values. While for the diffusive flux a linear interpolation is sufficient, the convective flux is discretised with the flux-limiting scheme. The linear interpolation of the diffusive flux $J_{i,j+1/2}$ at the cell boundary combined with the approximation of the spatial derivative in eq. 14 leads to a second-order scheme for the axial dispersion.

$$J_{i,j+1/2} = -D_i \frac{(y_{i,j+1} - y_{i,j})}{\Delta z}$$
$$F_{i,j+1/2} = \frac{v_{j+1/2}}{2}\left[(y_{i,j} + y_{i,j+1}) - sign(v)(1-\sigma_{i,j})(y_{i,j+1} - y_{i,j})\right]$$
$$\sigma_{i,j}(\theta_{i,j}) = \frac{\theta_{i,j} + |\theta_{i,j}|}{1+\theta_{i,j}} \qquad (15)$$
$$\theta_{i,j} = \frac{y_{i,j} - y_{i,j-1}}{y_{i,j+1} - y_{i,j}} \quad for\ v > 0$$
$$\theta_{i,j} = \frac{y_{i,j+2} - y_{i,j+1}}{y_{i,j+1} - y_{i,j}} \quad for\ v \le 0$$

The flow direction dependence on the ratio ensures that the stencil of the ratio is symmetric with respect to the position $j+1/2$ (in contrast to other published ratios), i.e. the numerator uses upstream values while the denominator is centred at the cell boundary. The flux limiter ensures that the higher order method is used in smooth regions of the solution while the stable first order upwind method is used around shocks. For example, for positive flow direction and values of the limiter $\sigma_{i,j}$ of 0, 1 and 2 the flux reduces to the first order upwind, second order central and first order downwind method, respectively. This numerical scheme has a number of benefits for the system considered. First, the FVM is inherently conservative so that even simulations with a few grid points conserve the mass in the system; this is particularly important for the closed DP-PSA system. Second, the flux-limiting scheme ensures that the shape of the solution along the column is qualitatively correct.

3.2 Solid phase spatial discretisation

In the case of the pore diffusion model in the adsorbent particles a discretisation scheme is required to discretise the diffusion equation. In a typical fast cyclic adsorption process the sorbate concentration can change considerably in parts of the adsorbent particle but usually only a small part of the particle actively takes part in the process.[15] The Orthogonal Collocation on Finite Elements Method is well suited to this case with large but stationary gradients.[16] The higher order of accuracy in comparison to most FVM allows the use of less grid points in the adsorbent particles and thus reduces the size of the resulting set of ODEs without compromising the accuracy of the solution.

3.3 Time integration

The SUNDIALS solver suite implements the variable-order, variable-step size Backwards

Differentiation Formulae and contains several direct and indirect linear system solvers.[13] The implicit solver can handle the algebraic equations generated from the OCFEM discretisation and for the flow velocities. Furthermore, the system contains effects with different time scales, e.g. axial dispersion and mass transfer kinetics, which are dominant during different parts of the cycle. Thus the variable step size of the integrator ensures that the largest time step which fulfils the accuracy requirements is used. For a conservative spatial discretisation scheme the error in the total mass balance of the system depends only on the accuracy of the time integration which can be controlled by tightening the absolute and relative tolerances. Figure S1 in the supporting information shows that the error in the total mass balance is controlled by the time integration tolerances thus verifying that the numerical scheme is conservative.3.4 Cycle simulation

The DP-PSA system like most adsorption processes is run in a cyclic manner until cyclic steady state (CSS) is reached. The solution at CSS is characteristic for the adsorption process; hence the system of equations has to be simulated to CSS for the analysis and optimisation of the adsorbent and process parameters, respectively. In the successive substitution approach the system is simulated analogous to the experimental system, i.e. the cycles are simulated one after the other and the state variables at the end of one cycle are used as the initial conditions for the next cycle. This approach provides information about the start-up and the time-evolution of the adsorption process. The CSS is reached once the state variables only depend on the spatial position in the system and the time relative to the start of the cycle. The employed condition for measuring the convergence to CSS is the root-mean square norm of the scaled deviations between the cycles k and k-1

$$E = \sqrt{\frac{\sum_{j=1}^{M}\left(\frac{x_j^k - x_j^{k-1}}{\max\left(\left|x_j^k\right|, atol\right)}\right)^2}{M}} < 10^{-4} \qquad (16)$$

where x_j^k is the vector of state variables, containing mole fractions, pressures, flow rates and sorbate

concentrations; atol and rtol are the absolute and relative tolerances of the time integration, respectively.

4. Experimental validation

The governing equations and numerical implementation are validated against experiments performed on a DP-PSA system filled with 13X zeolite adsorbent pellets. Initial single component runs with helium are used to determine the system volumes, i.e. the volume of the gas lines, the column volume and the piston volumes at the start of the piston strokes. Here it is assumed that helium is non-adsorbing but has access to the macro- and micropores. After establishing and validating the system volumes the system is run with a mixture of carbon dioxide and nitrogen.

The single-site Langmuir isotherms for CO_2 and nitrogen are calculated from the dual-site Langmuir isotherms from Xiao et al.[17] The kinetics for the mass transfer in the adsorbent pellets are under macropore diffusion control[6] and the effective pore diffusivity is given by

$$D_i^e = \frac{D_{p,i}}{\varepsilon_p + (1-\varepsilon_p)\frac{dq_i^*}{dc_i}} \tag{17}$$

where $D_{p,i}$ is the macropore diffusivity (see supporting information).[2] In the case of the LDF model the LDF coefficient is calculated from the effective pore diffusivity by

$$k_i = \frac{15 D_i^e}{r_p^2} \tag{18}$$

Figure 3 shows a comparison of the pressure profile over one cycle between the experiment and the simulation; the experiment conditions and parameters are given in table S1 in the supporting information. Both the LDF simulation and the macropore diffusion simulation (not shown) show very good agreement with the experimental data. The general cycle shape as well as the position and

magnitude of the pressure minima are simulated almost perfectly.

During the experiments the pressure drop across the column and the temperature inside the column were measured. The pressure drop in all cases studied was below 2.5 mbar which indicates that the no pressure drop model employed is suitable for these test cases. The largest temperature variation over one cycle from the cycle mean was less than ±2K. Thus the isothermal model employed is reasonably accurate and possibly an improved agreement with the position of the maximum in pressure in Fig. 3 could be obtained with a non-isothermal model. However, the mean temperature over one cycle increased by about 3K over the first hour of the experiment; this is most likely due to friction in the piston and will be investigated in a future publication.

5. Acceleration schemes

While the combination of the tailored discretisation schemes and the sophisticated DAE solver SUNDIALS generates an efficient and fast numerical scheme for the simulation of the DP-PSA system, the large number of different experiments combined with the potentially slow approach to CSS[5] justify the investigation into schemes which accelerate the approach to CSS.

The problem is approached from several angles. First, the simulation time for one cycle is reduced by employing node refinement similar to the work by Webley's group.[12] Second, the necessary number of cycles to reach CSS is reduced by using extrapolation methods for the calculation of the initial conditions and for the approach to CSS. Finally, these methods are combined.

5.1 Conservative node refinement

The use of the FVM in the discretisation of the fluid phase enables the use of successive node refinement as shown by Todd et al.[12] Briefly, the simulation is started with a small number of nodes. Once CSS is achieved the number of nodes is increased and the solution at the coarse grid is used to interpolate the starting conditions for the simulation run on the fine grid. This procedure is repeated (with the fine grid becoming the new coarse grid) until the variation in the solution for two successive grids is below a certain tolerance. Besides a reduction in the required simulation time this approach has the added benefit of providing a test on the required number of nodes to capture accurately the solution profile; depending on the process parameters the minimum number of nodes required to simulate accurately the solution changes.

Todd et al. use cubic-spline interpolation to calculate the nodal values for the finer grid. However, this interpolation scheme is not necessary conservative so that the mass balance might be violated. While a small error in the mass balance is acceptable for a standard PSA cycle with feed inlet and product withdrawal, this is unacceptable for a closed system such as the DP-PSA system. To address this shortcoming we employed two conservative interpolation methods as shown in figure 4. The simple interpolation method uses the cell value of the parent cell if the new cell lies completely in the parent cell and a linear interpolation of the values in two neighbouring cells if the new cell crosses a cell boundary. In the linear interpolation method all new cell values are linearly interpolated from the neighbouring parent cells. While the simple interpolation ensures both local and global conservation of each state variable, the linear interpolation method ensures only global conservation of each state variable and local conservation of the total mass in the gas phase, i.e. the mole fractions sum to one and the pressure stays constant. From figure 4 it is immediately clear that for the linear interpolation the mass of each state variable relative to the corresponding portion of the parent cell is not necessarily

conserved. However, the mass of each state variable is conserved over each pair of neighbouring parent cells and over the complete system.

5.2 Reduction of the number of cycles required to reach CSS

Since the convergence of the successive substitution approach to CSS is at best linear[9] several approaches which aim to increase the rate of convergence and thus reduce the number of cycles have been presented. Most of these methods use a Newton or quasi-Newton step to update the solution.[11, 4] However, while these methods increase the convergence rate they also incur a significant computational overhead, namely in the calculation of the Jacobian matrix for the Newton step. An alternative approach is the use of extrapolation algorithms. Kvamsdal and Hertzberg[18] compared the performance of a quasi-Newton approach with the Aitken and Muller extrapolation algorithms. While both of these extrapolation algorithms accelerate the CSS convergence they are either not stable enough or slower than the quasi-Newton method. Here we use the more sophisticated ε algorithm.[19] This algorithm was employed by Skelboe for nonlinear systems with a periodic steady-state solution.[20] Furthermore, he showed that the algorithm has a quadratic convergence rate under moderate conditions and is effective for systems with slowly decaying transients.

The extrapolation algorithm is given by

1. Set $e_0 = x^k$ where x^k is the state vector after the kth step of the extrapolation algorithm
2. Simulate q+2m cycles $e_1,\ldots,e_{q+2m}$ using successive substitution
3. Apply the ε algorithm to $e_q,\ldots,e_{q+2m}$:
    a. $\varepsilon_{-1}^r = 0, \quad r = 1,2,\ldots,2m$

b. $\varepsilon_0^r = e_r, \quad r = q,\ldots,q+2m$

c. $\varepsilon_{s+1}^r = \varepsilon_{s-1}^{r+1} + \left(\varepsilon_s^{r+1} - \varepsilon_s^r\right)^{-1}, \quad r = 0,\ldots,2m-1, s = 0,\ldots,2m-1$

4. Set $x^{k+1} = \varepsilon_{2m}^0$

The inverse in step 3c) is either the component-wise inverse in the scalar ε algorithm or the Samelson inverse $e^{-1} = e\left(e^T e\right)^{-1}$ in the vector ε algorithm. The two parameters q and m are problem dependent and will be determined from a series of simulations.

5.3 Restart with interpolation of the starting conditions

In the case of the analysis of the DP-PSA system and for parameter estimation in general many different simulation runs with only slightly varying parameter sets have to be performed. Usually only the solution at CSS is required so that it is entirely feasible to restart the simulation with initial conditions interpolated or directly taken from previous simulation runs. Here we use the solution values at CSS as the starting conditions for the simulation run with the next parameter set. Especially in the analysis of the different DP-PSA runs this mimics the way in which the experiments are run.

The combination of node refinement and the interpolation of the starting conditions requires a method to calculate the state variables on the coarse grid from the state variables on the fine grid. We calculate the average value of the state variables over the coarse grid and set the state variable to this value. This ensures that the mass is conserved, but decreases the prominence of maxima and minima.

6. Results and discussion

We apply the three acceleration techniques introduced in the previous section to the DP-PSA system with parameters given in Table S1 in the supporting information. First the techniques are used in isolation to establish their individual acceleration potential and finally the three techniques are combined.

6.1 Acceleration from conservative node refinement

The DP-PSA system from section 4 is simulated to CSS with and without conservative node refinement. Without node refinement the system is simulated to CSS with 41 and 61 nodes. After this we use the two conservative interpolation schemes with two steps from 21 to 41 and subsequently to 61 nodes. The simulation times are given in table 1.

Both conservative interpolation schemes with two steps, i.e. 21 to 41 and 41 to 61 nodes, converge to CSS substantially faster than the simulation without node refinement and 61 nodes. The speed-up is about 4.5 for the simple interpolation scheme and about 5.9 for the linear interpolation scheme. Furthermore, both simulations with node refinement are faster than the simulation without node refinement with only 41 nodes. While both interpolation schemes achieve a significant speed-up, the linear interpolation scheme which gives a smoother interpolation shows a faster convergence to CSS.

These speed-ups are slightly better than the ones achieved by Todd et al. which is most likely due to the differences in the adsorption systems studied. The DP-PSA system is enriching the light component in one piston and the heavy component in the other piston so that most of the cycles before CSS is reached are used to transport the two components across the column from the uniform initial conditions; thus the DP-PSA system is particularly suited for acceleration from conservative node

refinement.

6.2 Acceleration from the ε algorithm

The choice of the two parameters q and m, which affect the convergence properties of the ε algorithm, usually has to be based on *a priori* knowledge of the system.[20] The rapidly and slowly decaying transients govern the choice of the parameters q and m, respectively. The number of cycles to CSS for several combinations of q and m as well as for the scalar and vector ε algorithm is given in table S2 in the supporting information. Before the start of the first step of the ε algorithm we simulate four cycles by successive substitution. During these cycles rapidly decaying transients which are only present at the start of the simulation disappear and the overall number of cycles to CSS is reduced.

For all tested combinations of q and m the ε algorithm converges significantly faster than the subsequent substitution. In particular, for this test case the vector ε algorithm with q=3 and m=1 gives the fastest convergence: 24 cycles to CSS compared to 97 for subsequent substitution. This configuration is used to simulate the DP-PSA system with different parameters and the results are shown in table 2. In all cases tested the ε algorithm converged after a significantly lower number of cycles than the successive substitution simulation. A typical plot of the cyclic deviation E is shown in figure 5. This plot shows that the rate of convergence is higher than for successive substitution.

In contrast to Newton methods extrapolation methods are independent of the numerical integration method and require only the solution vector. Thus they can be applied to any simulation method and can be combined with the other two acceleration techniques presented in this paper.

Both extrapolation and Newton methods require a restart of the solver after each extrapolation step.

This entails re-initialising the initial conditions of the solver and setting the order of the Backwards Differentiation Formula to one. Thus after each extrapolation step the solver has to start with a small time step to compensate for the low order differentiation which reduces the solver efficiency. While this adds a small computational overhead for the DP-PSA system, it will not add extra overhead for general adsorption cycles, e.g. multi-step cycles, which usually have a solver restart at the start of the cycle anyway.

6.3 Acceleration through restart with interpolation of the initial conditions

To test the acceleration of the convergence to CSS due to the interpolation of the initial conditions we compare the number of cycles required to reach CSS for a simulation with uniform initial conditions (‘Cold start’) with a simulation started with the CSS solution for the system given in the previous section (‘Restart from base case’). This comparison is performed for variations in the stroke length, piston offset, mass transfer kinetics and equilibrium constant, which would be typical in simulations of either multiple experiments or numerical regression of the model parameters. Table 2 gives the number of cycles to CSS for the cold start and for the restart; the number of cycles to CSS is directly related to the simulation time required.

The results given in Table 2 show that the restart from a previously reached CSS significantly reduces the required number of cycles to CSS. For the variations in a single parameter tested, the speed-up varies from 1.35 for a 20° increase in the angle offset to 3.83 for a 10% increase in stroke length. However, for the cases where all four parameters are either increased or decreased by 10 %/ ° the speed-up is above 10. While other combinations gave only a speed-up around 2, this nevertheless shows that the restart from CSS conditions results in a significant reduction in the required number of

cycles to CSS. The magnitude of the simulated variations covers the usual step sizes in parameter estimation which thus can be expected to converge with about half the number of cycles.

Figure 5 in which the cyclic deviation for the cold start and restart case is plotted clearly shows that the convergence rate in both cases is almost the same; this behaviour was observed for all tested cases. Thus the convergence rate, i.e. the slope of the cyclic deviation plot, depends on the parameters and not on the initial conditions. However, the starting point obviously depends on the initial conditions. While the restart from the base case provided a speed-up of 2 in most cases, the speed-up in the case where all 4 parameters are varied simultaneously suggests that it might be possible to increase the speed-up even further. The CSS solution in this case is very close to the CSS solution for the base case. By analysing the effect of the various parameters and by then interpolating the initial conditions from several previous runs it might be possible to find similarly close initial conditions for arbitrary variations of the parameters; but this is beyond the scope of this contribution.

6.4 Combination of the three acceleration methods

The three acceleration methods presented in this paper can be combined to achieve even greater speed-ups. First, the initial conditions are interpolated from the previous simulation run. Second, from these starting conditions the system is simulated to CSS with a low number of grid points and the vector ε algorithm. Finally, the number of grid points is increased by the conservative node refinement strategy until the desired accuracy is reached. With this strategy the required simulation time for the four cases where one parameter is increased by 20 %/° is reduced by a factor between 8.5 and 10.8. Thus the acceleration can be combined to achieve an order of magnitude decrease in the required simulation time and allows to use non-linear parameter regression algorithms to determine model parameters from the simultaneous fit of multiple DP-PSA experiments.

7. Conclusion

In this contribution we have presented an efficient numerical simulator for DP-PSA systems. The mathematical model includes two models for the mass transfer kinetics, i.e. pore diffusion and LDF, which have a different computational complexity and are valid in different parameter regimes. The governing equations in the fluid and solid phase are discretised with tailored numerical schemes; thus reducing the computational cost while giving an accurate solution. The numerical simulations for both the pore diffusion and LDF model showed good agreement with experimental data.

We have presented three methods to accelerate the convergence to CSS: i) conservative node refinement; ii) ε algorithm; iii) interpolation of initial conditions. In the tested cases each of these acceleration methods reduced the computation time to CSS by a factor of 2 or more. Finally we combined the three acceleration methods and achieved a reduction in the simulation time by an order of magnitude. Applying these acceleration methods to the DP-PSA system will allow the efficient estimation of the adsorbent parameters from the experiments. A hierarchy of physical models is being developed as a further acceleration method, i.e. simulation of diffusion mass transfer models starting from the CSS of the LDF model.

Acknowledgements

The authors would like to dedicate this paper to Professor Giulio Sarti on the occasion of his 65th birthday. Professor Sarti has inspired us over the years with his work which has always combined advanced modelling and theory with experiments. We hope that he will enjoy this contribution which is aimed at coupling advanced modelling techniques to a novel adsorption experimental apparatus. One of the authors (MCF) would also like to thank Professor Sarti for his guidance during all her studies. Financial support from the EPSRC grants EP/F034520/1 - Carbon Capture from Power Plant and Atmosphere - and EP/I010939/1- FOCUS - Fundamentals of Optimised Capture Using Solids- is gratefully acknowledged.

Supporting information

Figure S1 showing the mass conservation of the numerical scheme. Tables S1 and S2 containing the parameters of the example case and the number of cycles to CSS for several configurations of the ε algorithm. Derivation of the effective pore diffusivity. This information is available free of charge via the Internet at http://pubs.acs.org/.

Notation

b_i	Langmuir constant, bar^{-1}
c_T	Total fluid concentration, $molm^{-3}$
D_i	Axial dispersion coefficient of component i, m^2s^{-1}
D_i^e	Effective pore diffusivity of component i, m^2s^{-1}
$D_{p,i}$	Pore diffusivity of component i, m^2s^{-1}
e_j	Vector of state variables in the ε algorithm
E	Cyclic deviation

J_i	Diffusive flux of component i, ms^{-1}
k_i	LDF coefficient of component i, ms^{-1}
L	Column length, m
L_p	Piston length, m
M	Total number of equations
N	Number of cells along the column
N_c	Number of components
P	Pressure, bar
q_i	Sorbate concentration of component i, $molm^{-3}$
q_i^*	Sorbate concentration at equilibrium of component i, $molm^{-3}$
$q_{s,i}$	Saturation capacity of component i, $molm^{-3}$
Q_i	Average sorbate concentration of component i, $molm^{-3}$
r_p	Particle radius, m
R	Column radius, m
R_p	Piston radius, m
S	Piston position, m
$S_{0,j}$	Start position of piston j, m
$S_{1,j}$	End position of piston j, m
t	Time, s
t_c	Cycle time, s
v	Interstitial flow velocity, ms^{-1}
V_D	Dead volume, m^3
$V_{p,j}$	Volume of piston j, m^3
x_j	Vector of state variables
y_i	Mole fraction of component i

$y_{i,pj}$ Mole fraction of component i in piston j

z Axial distance, m

Greek letters

ε Bed void fraction

ε_p Pore void fraction

$\theta_{i,j}$ Ratio of the solution vector for component i at node j

$\sigma_{i,j}$ Flux limiter for component i at node j

φ Piston offset

ω Angular frequency

References

(1) Gibbins, J.; Chalmers, H. Carbon capture and storage. *Energy Policy* **2008**, *36*(12), 4317.

(2) Ruthven, D. M. *Principles of adsorption and adsorption processes*; Wiley-Interscience, 1984.

(3) Keller, G. E.; Kuo, C. H. A. United States Patent 4354859, 1982.

(4) Jiang, L.; Biegler, L. T.; Fox, V. G. Design and optimization of pressure swing adsorption systems with parallel implementation. *Comput. Chem. Eng.* **2005**, *29*(2), 393.

(5) Todd, R. S.; Ferraris, G. B.; Manca, D.;Webley, P. A. Improved ODE integrator and mass transfer approach for simulating a cyclic adsorption process. *Comput. Chem. Eng.* **2003**, *27*(6), 883.

(6) Rajendran, A.; Farooq, S.; Ruthven, D. M. Analysis of a piston PSA process for air separation. *Chem. Eng. Sci.* **2002**, *57*, 419.

(7) Farooq, S.; Thaeron, C.; Ruthven, D. M. Numerical simulation of a parallel-passage piston-driven PSA unit. *Sep. Purif. Technol.* **1998**, *13*, 181.

(8) Singh, K.; Jones, J. Numerical simulation of air separation by piston-driven pressure swing adsorption. *Chem. Eng. Sci.* **1997**, *52*(18), 3133.

(9) Smith IV, O. J.; Westerberg, A. W. Acceleration of Cyclic Steady State Convergence for Pressure Swing Adsorption Models. *Ind. Eng. Chem. Res.* **1992**, *31*, 1569.

(10) Nilchan, S.; Pantelides, C. C. On the Optimisation of Periodic Adsorption Processes. *Adsorption* **1998**, *4*, 113.

(11) Ding, Y.; Levan, M. D. Periodic states of adsorption cycles III. Convergence acceleration for direct determination. *Chem. Eng. Sci.* **2001**, *56*(17), 5217.

(12) Todd, R. S.; He, J.; Webley, P. A.; Beh, C.; Wilson, S.; Lloyd, M. A. Fast Finite-Volume Method for PSA/VSA Cycle Simulation - Experimental Validation. *Ind. Eng. Chem. Res.* **2001**, *40*(14), 3217.

(13) Hindmarsh, A. C.; Brown, P. N.; Grant, K. E.; Lee, S. L.; Serban, R.; Shumaker, D. E.; Woodward, C. S. Sundials: Suite of Nonlinear and Differential/Algebraic Equation Solvers. *ACM Transactions on Mathematical Software* **2005**, *31*(3), 363.

(14) MacKinnon, R. J.; Carey, G. F. Positivity-preserving, flux-limited finite-difference and finite-element methods for reactive transport. *Int. J. Numer. Methods Fluids* **2003**, *41*, 151.

(15) Ahn, H.; Brandani, S. A New Numerical Method for Accurate Simulation of Fast Cyclic Adsorption Processes. *Adsorption* 2005, *11*(2), 113.

(16) Carey, G. F.; Finlayson, B. A. Orthogonal collocation on finite elements. *Chemical Engineering* **1975**, *30*, 587.

(17) Xiao, P.; Zhang, J.; Webley, P. A.; Li, G.; Singh, R.; Todd, R. S. Capture of CO_2 from flue gas streams with zeolite 13X by vacuum-pressure swing adsorption. *Adsorption* **2008**, *14*(4-5), 575.

(18) Kvamsdal, H. M., & Hertzberg, T. Optimization of PSA systems—studies on cyclic steady state convergence. *Comput. Chem. Eng.* **1997**, *21*(8), 819.

(19) Wynn, P. On a Device for Computing the em(Sn) Transformation. *Mathematical Tables and Other Aids to Computation* **1956**, *10*(54), 91–96.

(20) Skelboe, S. Computation of the periodic steady-state response of nonlinear networks by extrapolation methods. *IEEE Transactions on Circuits and Systems* **1980**, *27*(3), 161.

Figures

a)

b)

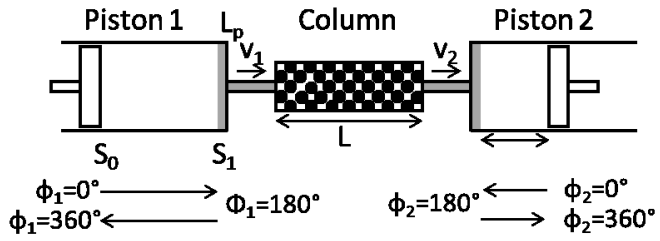

Figure 1: a) DP-PSA system b) Schematic of the system

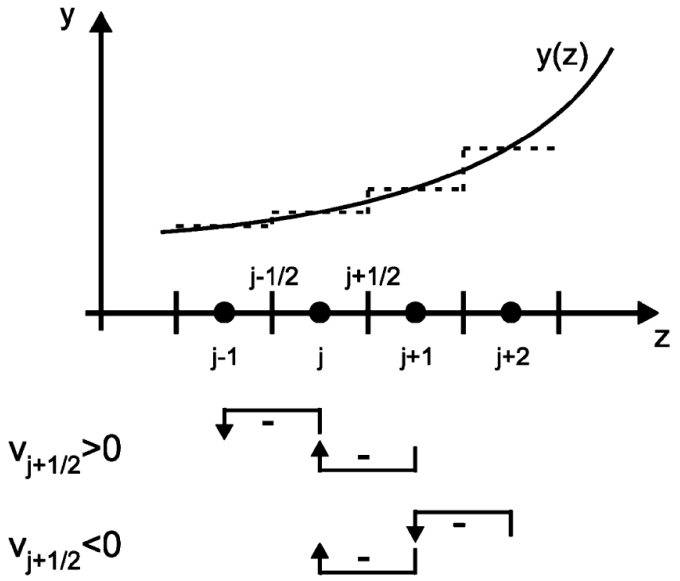

Figure 2: Schematic of the node based finite volume method. The dashed lines in the graph show the average value over each cell. The bottom of the figure shows the support of the flux limiter through the cell boundary j+1/2 for positive and negative flow.

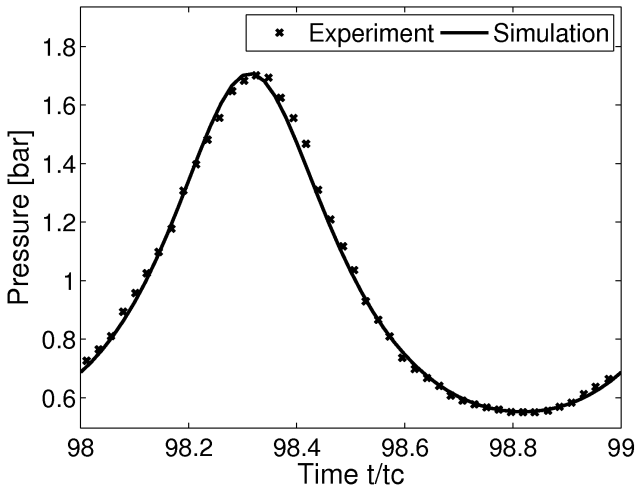

Figure 3: Comparison between the experiment and the LDF simulation of a CO_2 /N_2 run for a 10 s cycle on 13X in the DP-PSA system for the conditions given in table 1.

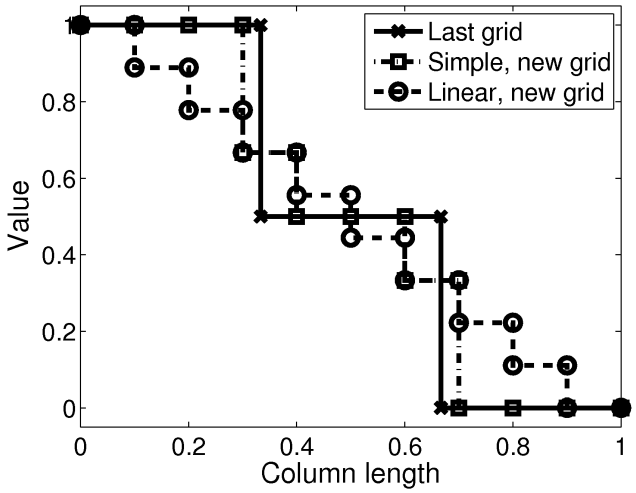

Figure 4: Schematic of the two conservative interpolation schemes.

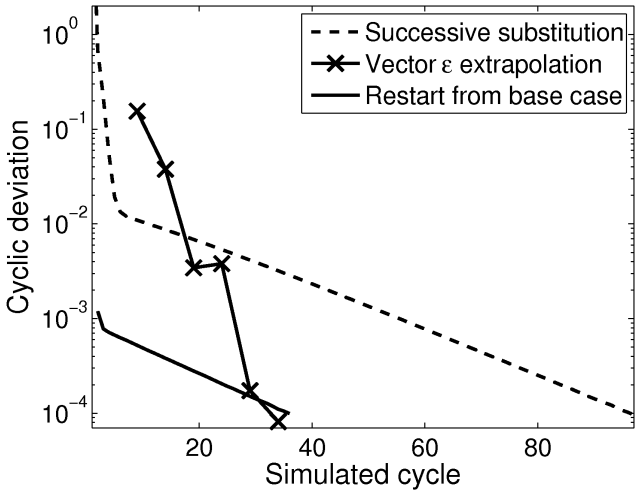

Figure 5: Comparison of convergence to CSS for subsequent substitution, vector ε algorithm and restart from the base case. The stroke length in piston 1 is increased by 20% in relation to the base case.

Tables:

Table 1: *Simulation time for the DP-PSA system with and without conservative node refinement. The simulation time is given as a percentage of the longest simulation time, i.e. the simulation with N=61 and no node refinement.*

	N=21	N=41	N=61	Total
No node refinement			100%	100%
No node refinement		35.9%		35.9%
Simple node refinement	8.1%	6.5%	7.2%	21.8%
Linear node refinement	8.3%	4.1%	4.6%	17.0%

Table 2: Comparison of the number of cycles required to reach CSS for successive substitution with cold start, the vector ε algorithm and restart from the base case.

Case	Cold start	Vector ε algorithm, q=3, m=1	Restart from base case
$(S_{1,1} - S_{0,1}) + 10\%$	92	39	24
$(S_{1,1} - S_{0,1}) + 20\%$	88	34	36
$(S_{1,1} - S_{0,1}) - 10\%$	103	34	33
$\Phi_1 + 10^{\circ}$	88	34	51
$\Phi_1 + 20^{\circ}$	81	29	59
$\Phi_1 - 10^{\circ}$	108	44	63
$k_1 + 10\%$	100	34	49
$k_1 + 20\%$	103	34	62
$k_1 - 10\%$	95	39	43
$b_1 + 10\%$	108	44	52
$b_1 + 20\%$	119	39	70
$b_1 - 10\%$	87	39	41
All + 10 %/$^{\circ}$	95	39	9
All - 10 %/$^{\circ}$	100	34	8